KfK 3330
Juli 1982

A Brief Review of Transition Phase Technology

W. Maschek
Institut für Neutronenphysik und Reaktortechnik
Projekt Schneller Brüter

Kernforschungszentrum Karlsruhe

KERNFORSCHUNGSZENTRUM KARLSRUHE

Institut für Neutronenphysik und Reaktortechnik
Projekt Schneller Brüter

KfK 3330

A Brief Review of Transition Phase Technology

Werner Maschek

Kernforschungszentrum Karlsruhe GmbH, Karlsruhe

Kernforschungszentrum Karlsruhe GmbH
ISSN 0303-4003

Abstract

A brief review of important phenomena pertaining to the transition phase is given. Special emphasis is laid on the recriticality issue as this process has the potential for energetic disassemblies of the already disrupted core configuration. Questions related to recriticalities such as removal of fuel from the core region, freezing and blockage formation, the behaviour of molten/boiling fuel-steel pools (flow regimes, heat transfer etc.) are discussed.

Eine kurze Übersicht der Technologie der Übergangsphase

Zusammenfassung

Es wird eine kurze Übersicht wichtiger Phänomene der Übergangsphase gegeben. Dabei wird besonderes Gewicht auf die Rekritikalitätsfrage gelegt, da dieser Prozeß das Potential für eine energetische Zerlegung des bereits weitgehend zerstörten Reaktorkerns besitzt. Mit Rekritikalitäten zusammenhängende Fragen wie die Entladung des Kernmaterials, Gefrier- und Blockadeprozesse, das Verhalten von geschmolzenen/siedenden Brennstoff-Stahlpools (Strömungsform, Wärmeübergang etc.) werden diskutiert.

This report is an extended version of a paper given at Ispra Courses Seminar: Multiphase Processes in LMFBR Safety Analysis, 29 March - 2 April 1982.

Table of Contents

		page
I.	Introduction	4
II.	Phenomena Related to the Transition Phase	9
	II.1 The Recriticality Potential	9
	II.1.1 The Occurrence of Recriticalities	9
	II.1.2 Modes of Recriticality	10
	II.1.3 Excursion Energetics Decreasing and Increasing Phenomena in Fuel/Steel Pools	13
	II.1.4 Pressure Driven Recriticalities	15
	II.2 Fuel Removal from the Core	17
	II.2.1 Paths for Fuel Removal from the Core	17
	II.2.2 Experimental and Theoretical Information about Blockage Formation	18
	II.3 Flow Regimes in Boiling Pools	24
	II.4 Heat Transfer from Internally Heated Pools	29
III.	Mechanistic Analysis of the Transition Phase	38
IV.	Conclusions and Final Remarks	41
V.	References	42
VI.	Nomenclature	49

List of Figures

		page
Fig. I.1	Phase Diagram for Core Disruptive Accidents (SNR-300)	5
Fig. I.2	Principal Sketch of Core Configuration during Pretransition Phase	7
Fig. I.3	Principal Sketch of Core Configuration during Transition Phase	8
Fig. II.2.2.1	Initial Temperature Map for Initially Molten UO_2 Contacting Initially Solid Stainless Steel	20
Fig. II.2.2.2	Fuel Freezing Models	23
Fig. II.3.1	Flow Regimes in a Boiling Fuel/Steel Pool	26
Fig. II.3.2	Pool Average Void Fraction Measurements	28
Fig. II.4.1	Natural Convection to a Vertical Surface Adjacent to a Volume Heated Boiling Pool	30
Fig. II.4.2	Correlation of Local Heat Transfer Data from Volume-Boiling Pools in Bubbly Flow- $Ra^x \leq 2 \cdot 10^{11}$	34
Fig. II.4.3	Correlation of Local Heat Transfer Data from Volume-Boiling Pool-$Ra^x > 2 \cdot 10^{11}$	35
Fig. II.4.4	Lateral Boundary Heat Transfer Correlations from Volume-Boiling Pools	36
Fig. III.1	Nuclear Power Trace of Mechanistic SAS3D/SIMMER-II Calculation	40

List of Tables

		page
Tab. II.3.1	Values of the Stability Parameter K	26
Tab. II.4.1	Summary of Local and Average Correlations for Heat Transfer from Volume Boiling Pools	37

I. INTRODUCTION

Hypothetical core disruptive accidents (HCDAs) have played an outstanding role in Liquid Metal Fast Breeder Reactor (LMFBR) safety evaluations. Since the fast reactor core is not assembled in its most reactive configuration, redistribution processes of the core materials (fuel/steel/sodium) during core disruption have the potential of leading to severe nuclear power excursions. Consequently, not only are extreme precautions taken to prevent conditions leading to core disruption but also major efforts are being devoted to assess the consequences from the hypothetisized occurrence of such conditions.

The safety concept of FRG Fast Breeder Reactors (SNR-300 or future SNR-1300) is based on the multiple barrier concept and on several levels of safety design. The first level of safety design prevents the occurrence of fault initiation and assures low probability of occurrence for accident initiations. The second level prevents the propagation of faults into serious core accidents and the third level assures adequate mechanical/thermal response of the reactor system against extremely unlikely severe accidents, thereby limiting the release of radioactivity to acceptable low limits. On the first and second level of safety design a criterion of less than 10^{-6}/a for loss of coolable core geometry is met e.g. for SNR-300 by using a plant protection system with two independently and diversely acting shutdown systems /1/.

Due to this low probability level of less than 10^{-6}/a core disruptive accidents are called hypothetical to convey some flavour of the low probability or even incredibility.

Accident analyses performed for SNR-300 mainly deal with the loss of flow accident (pump trip with failure to scram - LOF) which can be shown covers in its possible energetics all other accident initiators as e.g. the transient over power (insertion of uncontrolled positive reactivity with failure to scram - TOP (steep ramp rates larger than 4 ¢/sec can be excluded)) which has in addition an even lower probability of occurrence.

The now rather complete picture of the potential core disruption accident paths must be regarded as a significant progress in LMFBR safety research.

It was achieved by experimental and theoretical research of the fundamental physical processes and by the development of various accident analysis tools. The accident sequence may be best described in terms of the so-called accident phases. Each phase is distinguished by a set of several physical key processes which evolve during accident progression.

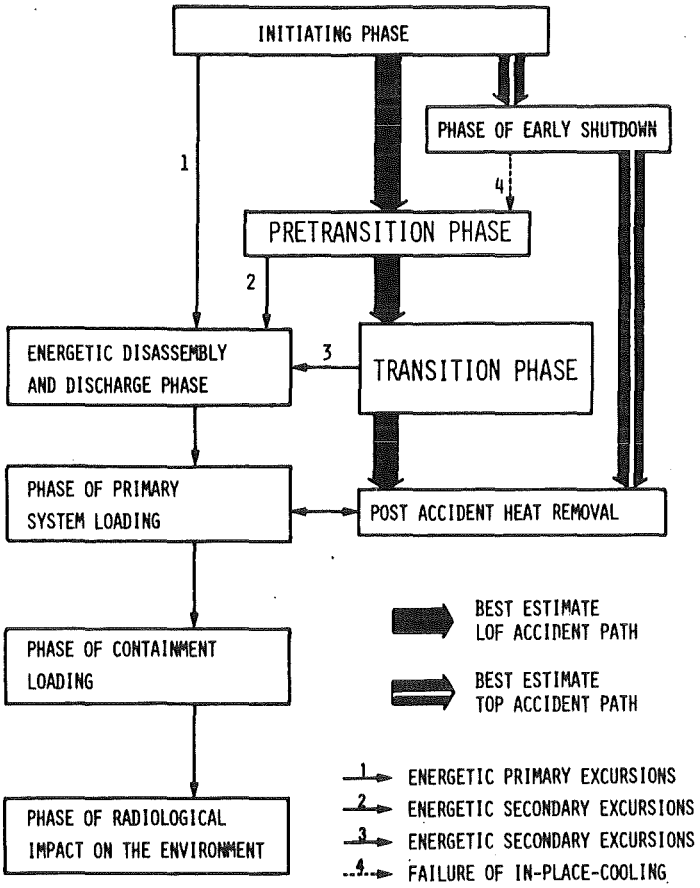

Fig. I.1 Phase Diagram for Core Disruptive Accidents (SNR-300)

Early studies of fast reactor accidents emphasized the analysis of energetic excursions where the accident initiation ended by a violent core disassembly on the milliseconds timescale. As a result especially of the analyses related to FFTF in 1974 /2/ it was recognized that the initiation phase need not terminate energetically. Instead, an alternate accident progression path was realized where sufficient negative neutronics feedback prevents a violent disassembly but leads to a gradual melting and core disruption and the formation of pools of molten/boiling fuel and steel on a

seconds timescale. This accident phase that involves a grossly disrupted core where substantial motion of molten fuel has occurred was called the Transition Phase. The transition from the intact geometry of the initiation phase to the grossly disrupted state of the transition phase is sometimes called the Pretransition Phase. This paper deals with both phases.

A major factor in the analysis which originally led to the introduction of a transition phase is the low sodium void coefficient characteristic to the FFTF. However it has been demonstrated /3/ that with best estimate modelling and parameters also reactors with higher void coefficients such as the SNR-300 can be expected to enter the transition phase.

It is emphasized that this paper mainly reflects the work done for SNR-type reactors in this field. Processes and phenomena discussed may be different or more/less dominant in other types of reactors.

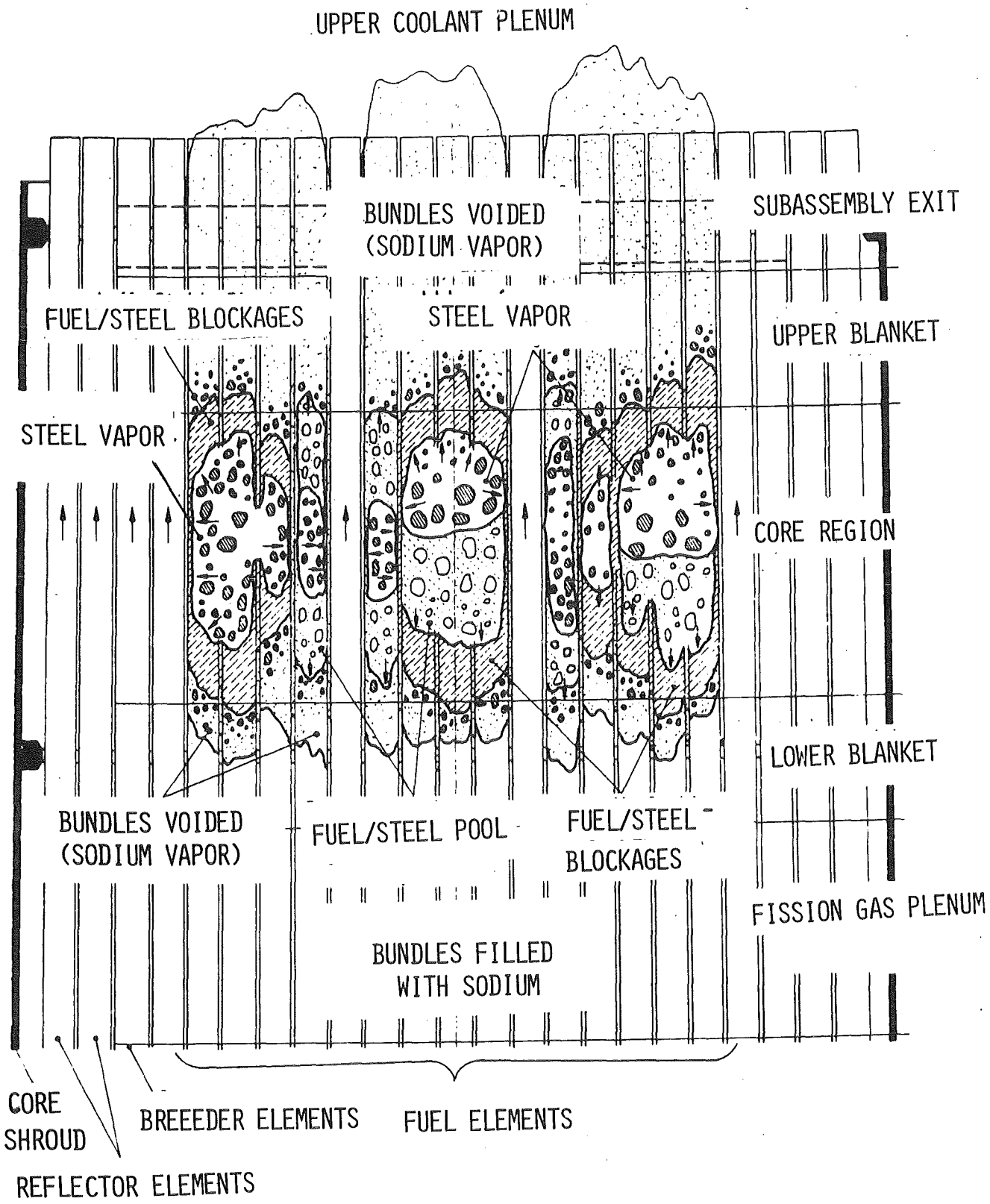

Fig. I.2 Principle Sketch of Core Configuration during Pretransition Phase

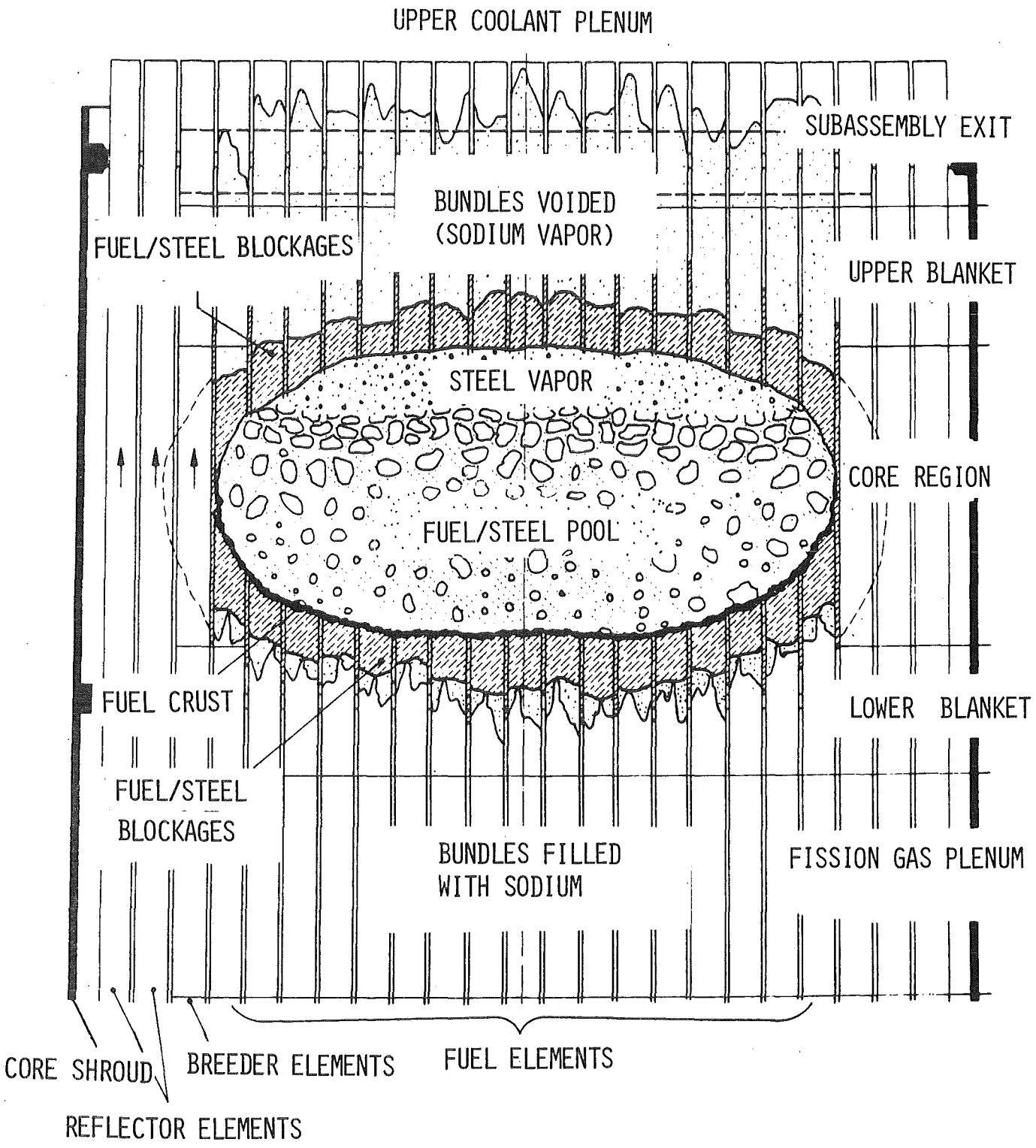

Fig. I.3 Principle Sketch of Core Configuration during Transition Phase

II. PHENOMENA RELATED TO THE TRANSITION PHASE

II.1 THE RECRITICALITY POTENTIAL

II.1.1 The Occurrence of Recriticalities

As the fuel is not in its most reactive configuration, redistribution and compaction processes of the fuel mobilized by the primary neutronic burst during the initiation phase (triggered by sodium boiling and voiding) may result in a new critical configuration (recriticality) which involves a secondary nuclear excursion. Thus also during the mild meltdown phases (pretransition/transition phase) there exists the potential for energetic disassembly of the already disrupted core configuration (Paths 2, 3 in Fig. I.1). The question of a recriticality potential is related to the question of fuel penetration and/or blockage formation by frozen core materials in colder core or blanket regions. Assuming that during pretransition phase core material could be continuously discharged from the individual subassemblies accident analysis shows that the mobile core material gets lost from the active region with mostly intact hexcan-structure finally leaving the reactor highly subcritical. The ejected fuel settles in the tank after granulation on contact with sodium. Finally after core pressure has decayed reentering sodium cools the disrupted rest structures.

If on the other hand only little fuel is lost and is trapped in the axial/radial blankets by fuel freezing processes the core region gets sealed and most of the fuel inventory is kept in this confined region ("bottled up pool"). Before hexcan meltthrough the material motion in the individual subassemblies is strongly incoherent preventing high reactivity insertion rates and recriticality triggered energetic disassemblies (Path 2 - Fig. I.1). Nuclear heating and neutronic/fluiddynamic coupling leads to a progressive mobilization of fuel and tuning of previously incoherently behaving material. Hexcan destruction eventually leads to large connected pools or even a whole core pool. By this the conditions for a severe recriticality event are met: large parts of the fuel inventory can move coherently (Path 3 - Fig. I.1). If it is a compactive motion even prompt critical reactivity states could be reached which implies a severe nuclear power excursion leading to thermal and mechanical disruption of the

blockages and discharge of core material into the sodium pool surrounding the core. The resulting nuclear subcritical configuration again will be cooled by inflowing sodium.

If hexcan melting leads to a dropping of the upper blanket into the pool region (see Chap. III) the fuel/steel mixture will be diluted and quenched by the depleted blanket uranium. The further course of the accident is characterized by downward melting through the lower blanket/plenum structures.

If the initiation phase of the accident directly enters into an energetic disassembly /3/ massive fuel discharge from the core leaves no potential for recriticalities for accident path 1 in Fig. I.1.

II.1.2 Modes of Recriticality

The assessment of recriticality focuses mainly on the evaluation of fuel motion. The potential driving forces for fuel motion are gravity, fuel/steel/sodium vapour and fission gases. In addition it is important to consider the presence and motion of other materials which may make up the core internals as steel, sodium, control-, blanket material and fission products. The motion of these materials or their presence e.g. steel in the forms of hexcans can strongly influence the reactivity swings (ramp rates) during fuel motion and also influences the thermal energy deposition and conversion to mechanical energy in the case of a power excursion.

One of the most important issues dealing with the core materials during the transition phase is the vicinity of the fuel melting point (3060 K) and the steel boiling point (3080 K) /8/. Thus molten fuel will be accompanied by boiling steel which leads to a dispersion of the molten core-materials if enough energy production is provided by fission and decay heat. This fuel dispersion leads to highly subcritical states. The question of recriticality deals mainly with processes which disturb this dispersion and boilup and lead to fuel compaction.

Further below a list is given of processes which have the potential to initiate a fuel compaction and recriticality during the pre- and transi-

tion phase. Recriticality modes listed under pre- and transition phase can also partly occur in both phases. Simply due to the power - surface/volume ratio e.g. pool collapsing in the pretransition phase would be more dominated by heat losses and melt-in processes whereas pool collapsing in the transition phase would result more from self-pressurization etc.

Pretransition Phase

o Recompaction of disrupted fuel in intact hexcan structure

The primary excursion leads to an axial breakup of fuel pins leaving still intact pin stalactites hanging above core midplane. Loss of pressure support from below allows gravity slumping and fuel compaction. Incoherence effects caused by still intact hexcans strongly mitigate reactivity insertion rates.

o Pool collapse

Collapse of single subassembly pools (if they exist in a boiled-up state at a higher power level) by high heat losses, cold molten steel entrainment from subassembly hexcan melting etc. Incoherence of fuel motion limits reactivity insertion rates. Pool collapse tendency by heat losses decreases with pool size.

- High heat losses

If heat losses to the structure surroundings are too high, not enough energy for steel vaporization will be available for pool dispersal. A decisive role is played by the existence or non-existence of isolating fuel crusts. If a stable fuel crust exists on the pool boundaries heat losses would be drastically diminished (see Chap. II.2).

- Melt-in of cold materials

Steel structure (subassembly ductwall) melting or fuel crust breakup and steel intrusion into the pool can quench the pool. The same may occur with melt-in/fall-in of blanket pellets. By this process the reactivity level, however, drops drastically and compaction processes lead to diminished reactivity ramp rates (see Chap. III).

o Mixing of enrichment zones

In homogeneous two-zone cores total mixing of the core zones after hexcan meltthrough has a reactivity potential of 10 - 20 $. Axial dispersion and blockage formation before hexcan melting and mixing, however, lead to highly subcritical reactivity states balancing this reactivity potential. In addition total fuel mixing could only be achieved on a seconds timescale.

Transition Phase

o Pool collapse

For a dispersed boiling pool of fuel and steel in a nuclear subcritical configuration various mechanisms have been postulated for collapsing and leading to recriticality.

- Selfpressurization of pool

  Although it is desirable that heat losses to the structures surrounding the pool are limited to provide sufficient energy for steel vaporization, a heat sink above the pool is required to condense steel vapor. If vapor condensation is hampered e.g. by noncondensible gases (fission gas) the pool will become adiabatic and will pressurize. The accompanied drop in vapor velocity may lead to pool collapse (see Chap. II.3).

- High heat losses
  (see pretransition phase)

- Melt-in of cold materials
  (see pretransition phase)

- Fuel/steel separation

  The lighter steel will exhibit a tendency to rise above the heavier fuel thus leading to a separation of the energy and vapour producing source. However dynamic pool behaviour will probably ensure mixing.

o Coherent fuel motion

Dynamic motion of fuel itself can recompact into critical configuration

- Sloshing fuel motion

  Although pool behaviour is dispersive, oscillatory type motions eventually result in neutronic power bursts where material that has moved to the core periphery reverses motion and collects in a compactive way (see Chap. III).

- Autocatalytic material motion

  In reactor cores with high enrichment and special design (very tall, pancaked etc.) material motion to the core periphery will not lead to a decrease but an increase in reactivity. Thus an excursion directly drives another (more severe) excursion (see Chap. II.1.3).

o Reentry of previously ejected core material

Classical mode of recriticality where fuel discharged due to the primary power burst and frozen in the axial blankets remelts and recollects in the core region. Incoherency effects at reentering and co-entering blanket material diminishes reactivity insertion rates.

o Separation of control rod material

As HCDA assumes a non-scram condition, only limited CR material (B_4C) is available for separation in a pool. Effects like buoyancy driven separation of B_4C lead only to small reactivity insertion rates.

It should not be surprising that no typical reactivity ramp rates are given for the various processes for assessing the energetics of possible excursions. However, calculations show that the thermal energy (and by this mech. energy) levels resulting from recriticality are affected by both ramp rates and responsiveness of the configuration that generated the ramp rate. Recriticality mode and its severity also depend on the specific reactor design. Therefore it is our opinion that only giving ramp rates oversimplifies the problem and may lead to erroneous conclusions.

Due to the largely intact hexcan structure reactivity ramp rates and energetics of the pretransition phase are usually lower than those of the transition phase. Giving typical bounds for the mechanical energy release (determined by isentropic expansion of the hot fuel vapour to the cover gas volume) for SNR-300, the pretransition phase energetics will range between 0 - 50 MJ and the transition phase between 0 - 100 MJ.

II.1.3 Excursion Energetics Decreasing and Increasing Phenomena in in Fuel/Steel Pools

The energetics-potential of nuclear power excursions triggered by compactive material motion can be reduced by several effects that limit reactivity ramp rate insertion.

- Early fuel discharge and incomplete blockage formation reduces the amount of mobile fuel that can participate in compactive motion and limits the amount of core involvement.

- Reduction of the fuel enrichment by dilution with blanket material leads to both a reactivity drop and a decrease in the neutronic/fluiddynamic coupling.

- Incoherence of material motion (3 dim.) caused by existing core structures (hexcan-structure, control rods, fuel-, blanket-subassemblies (heterogeneous core) etc.) strongly limit accumulation of high reactivity ramp rates.

The energetics of an excursion may be enhanced by a so-called autocatalytic effect. Autocatalytic effects can be characterized that they drive themselves over a feedback loop. Within the framework discussed here that would mean that fuel motion or thermohydraulic effects lead to a reactivity and nuclear power increase which itself enhances fuel motion or the thermohydraulic effect and gives rise to further reactivity/power increase.

Within the framework of recriticality analyses mainly two effects have to be discussed.

- Autocatalytic material motion.
  Core material reconfiguration triggered by a nuclear power excursion directly leads to a new critical or even prompt critical configuration. Material motion into core peripheries does not lead to nuclear shutdown but to reactivity increase. These effects are discussed in some length in /9/. These effects can occur in specially designed cores but do not exist for SNR-300 type reactors /10/.

- Assuming a bubbly flow regime (see Chap. III.3) during the fuel heat-up during a severe nuclear power excursion the bubbles may collapse either by thermal expansion of fuel or by insufficient material evaporation into these bubbles. This leads to a decrease in neutron streaming and an increase in reactivity. The reactivity potential is dependent on the bubble diameter. Bounding case studies with large bubbles reveal a reactivitiy potential of 1 - 2 $ that is additionally available during a prompt critical excursion from the streaming process /7, 10/. However, analysis shows that only a small percentage of the available reactivity potential is added during an excursion.

Another energetics increasing effect results from the loss of volatile precursors from the boiling fuel/steel pool by evaporation processes. The reduction of precursors leads from the neutronics viewpoint to an increase in the severity of a nuclear power transient and to a decrease of heat generation for pool boilup. However analysis shows /11/ that precursor evaporation has no decisive influence on accident energetics.

II.1.4 Pressure Driven Recriticalities

Sodium vaporization on fuel/steel contact (Fuel Coolant Interaction - FCI) could be conceived to trigger both dispersive and compactive fuel motion. It strongly depends on the actual situation and core configuration which mode may prevail.

Pressure driven recriticalities have been discussed mainly within the framework of (a) direct fuel flow reversal and reentry after injection of fuel into the upper/lower core-bundle structure, (b) delayed reentry of fuel from remelting blockages in the upper/lower bundle structure, (c) fuel flow reversal after blockage melting and fuel discharge from a "bottled up" pool, and (d) sodium leak into the "bottled up" pool and pool pressurization /16, 45/.

Simple idealized calculations assuming sustained pressure build-up after FCI in the upper core structures revealed the existence of a potential for large reactivity ramp rate insertion /12/. For this reason a specific experimental program has been set up, the Upper Plenum Injection (UPI) Tests, to investigate the influence of sodium in a bundle structure on fuel motion and redistribution. Several pressure driven, fuel insertion experiments have been conducted with uranium thermite and simulant materials in 37 pin wire wrapped bundles /13, 14/. The experiments have been performed with the bundle full, half-full and empty of sodium coolant. Measurements and post-test examination of the bundles showed that the sodium coolant had no significant effect on the final disposition of the fuel. No forces capable of reversing the flow of the fuel and recompacting it were observed. Only local, small-scale FCI pressure spikes (halfwidth < 1 msec) occurred during the tests which are not capable of reversing material motion. The dominant processes seen were fuel quenching and freez-

ing. It has been criticized that the void fraction of the first UPI tests was very high (98 %). Though experiments with simulant fluids show no significant effect of void fraction or flow regime this point needs further clarification*. Nevertheless the contact mode - two-phase fuel with liquid sodium - seems to be the dominant mode when the hot fuel/steel mixture is ejected from the core region. Stability considerations render the contact of a dense liquid fuel slug with sodium unlikely when fuel is accelerated and driven out of the core region. Thus a necessary condition for FCI, liquid-liquid contact is prevented by inherent instability and the accompanying fuel/steel/sodium vapors and fission gases during fuel motion.

Pressure driven recriticalities from fuel reentry in constrained geometry or after blockage remelting in a molten/boiling pool will also be strongly mitigated by incoherency effects. For generating significant reactivity insertion rates a massive fuel reentry must occur with 100 kgs and more of fuel involved. As one single bundle contains between 20 - 30 kg and fuel is distributed up and downward in the bundle and partly frozen in the upper and lower axial blankets it is obvious that such high reentering masses imply a large number of bundles participating in reentry. For obtaining high ramp rates this fuel must move (fall) coherently on a time interval of milliseconds. Otherwise reactivity ramp rates would be drastically diminished /7/.

In the case of core material ejection from a whole core pool into the upper plenum an FCI in the above unconstrained geometry (in SNR-300) would quickly relieve pressure (only $\sim$ 4 m sodium above) and will lead to a slowdown of fuel/steel ejection (self-limiting process).

Massive leak-in of sodium through blockages and pressurization of the bottled up pool below could theoretically lead to pool compaction and sloshing motions as discussed in Chap. II.1.2 /16/. However massive penetration of blockages that could confine boiling pools and which are at temperature levels well above the boiling point of sodium can be excluded. Thus sodium leak-in should only be expected after gross fuel/steel dis-

---

* Recent results with prototypic materials and lower void fractions however confirm these results /15/.

charge processes, blockage opening and pressure relief in the neutronically subcritical pool region. Preliminary experiments concerning pressure driven pool collapses are reported by Koontz /17/ where two simulant fluids were brought into contact to model sodium pressurization and pool collapse. The collapse rates in this simulant experiment were not very fast. However these experiments would need further evaluation and testing.

II.2 FUEL REMOVAL FROM THE CORE

II.2.1 Paths for Fuel Removal from the Core

As discussed in Chap. II an essential condition for entering the energetic recriticality path is the formation of axial and radial fuel/steel blockages around the active core region which limits the material discharge from the core and prevents fast achievement of permanent subcriticality. Thus the question of material freezing in colder structures is a key issue of pre- and transition phase analysis determing which course the accident will take.

For fuel blowdown and discharge from the core region various paths exist which may become operable at different time-scales of the accident sequence. Thus scale and timing of fuel removal determine the accident evolution:

- o Blowdown through intra-subassembly structure

  This is the first achievable and direct path for fuel removal. This removal path has therefore been extensively investigated both analytically and experimentally.

- o Blowdown between hexcans

  After melting of the subassembly duct walls this fuel removal path becomes available. Penetration can be expected both axially and radially into the upper/lower and radial blanket structure. Comparing the hydraulic diameter, it is about twice that of the intra-subassembly paths. Thus the gaps between the subassembly duct walls are also potential paths for fuel removal.

o Subassembly head tear-off

Under high pressure loads massive core material discharge could also be initiated by a mechanical failure of the upper core structures.

o Blowdown through control rods or special dummy elements

Fuel removal through these paths is strongly design dependent. However if such paths exist, they could give large openings for fuel removal as the hydraulic diameters are about 10 times that of the intra-subassembly paths. These removal paths become operable rather late in accident progression.

It should be mentioned that the nature of the blockages depends both on the specific accident phase and on the reactor design. Low void cores (cores with small positive sodium void coefficient) favour early clad motion. Early blockage formation during the pretransition phase will be mainly due to steel freezing (fuel becomes trapped in the core) whereas blockages formed during the transition phase will consist of both steel and fuel. For higher void cores steel and fuel become mobile nearly simultaneously thus also blockages are built up of both constituents.

II.2.2 Experimental and Theoretical Information about Blockage Formation

The experimental and theoretical effort in studying blockage formation is mainly directed to intra-subassembly fuel motion and freezing. Freezing of a liquid with change of phase and moving boundaries has been discussed in the literature for over two decades. However the conventional freezing problems are solved mostly under very idealized conditions. In the reactor situation the process of freezing is strongly and mutually dependent on various parameters as geometry, heat transfer with change of phase, internal heat generation, flow in channels with variable cross sections, pressure, flow velocity, temperatures, wall temperatures, turbulence, crust stability, ablation of molten material and mixing etc. As a detailed description of freezing involving all these processes is extremely complicated this problem has been approached with different degrees of approximation.

An essential issue in discussing fuel freezing is the formation of solid fuel crusts. A characteristic of fuel freezing on solid steel is that the

surface of the underlaying steel will melt upon contact with the fuel that forms a solid crust simultaneously, if the initial temperature of the steel wall is sufficiently high. For a given steel temperature T_s fuel crust formation without steel melting can be expected below the line $T_f \tilde{=} - 2.64T_s + 5500$ [K] /18/. Using not the constant room temperature properties in steel but accounting for the increase in both the thermal diffusivity and conductivity of steel as the melting temperature is reached this line shifts to higher steel temperatures $T_f \tilde{=} - 3.12T_s + 7200$ [K] /23/. Above these lines fuel crust formation and simultaneous steel melting are calculated. At very high fuel/steel temperatures both components will be liquid on contact. The presence of an isolating crust could reduce the heat transfer driving temperature difference from about 1500 K to approximately 100 K leading due to this isolation to extensive penetration lengths by the flowing material. With no fuel crust steel melting, entrainment of molten steel and rapid freezing of the fuel/steel mixture occurs.

In considering heat exchange between the molten fuel stream and steel structure the thermal and mechanical stability of the growing fuel crust is a most important concern. Theoretical analyses of Epstein et al. /19/ showed that a critical velocity v_{crit} of flow could be derived where one must expect mechanical breakup of the crust by the dynamic pressures exerted by the flowing material. The critical velocity is high for low initial wall temperatures and decreases rapidly as steel wall temperature increases. For molten fuel flowing in a tube with a temperature of 3500 K and a steel wall temperature of 900 K the critical velocity of the UO_2 is about 30 m/sec, for 1300 K v_{crit} is only $\sim$ 8 m/sec.

Concerning thermal stability it is stated /19/ that in the presence of molten fuel superheat ($T > T_{melt}$) the growth of the frozen fuel layer comes to a stop when the conduction heat flux into the steel channel wall balances convection from the flowing fuel. At this instant, the frozen layer will begin to melt.

Concerning the question of crust stability numerous experiments with simulant fluids have been performed /20, 21/ under different experimental conditions, as crust stability in pool geometry (see Chap. II.3), in tube flow and liquid jet impingement (hot water on frozen octane).

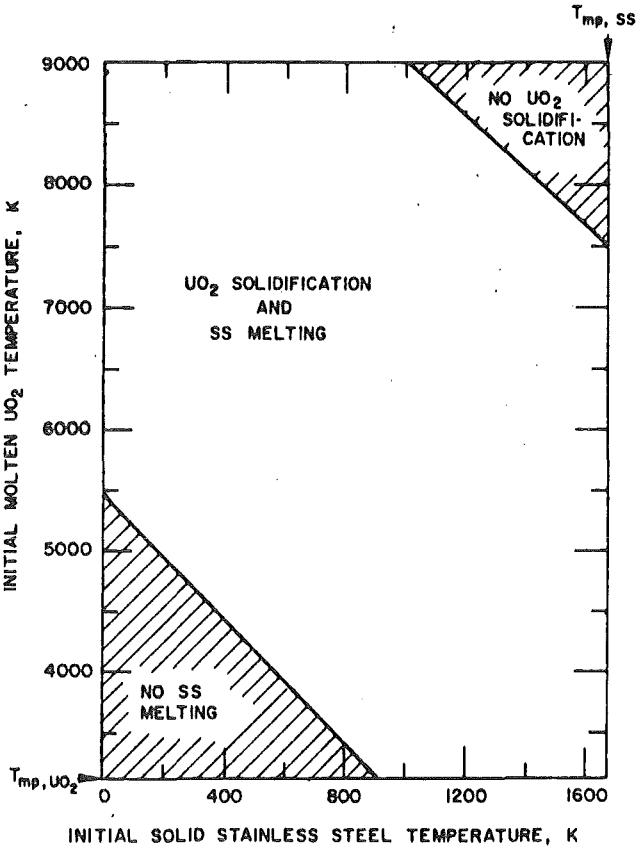

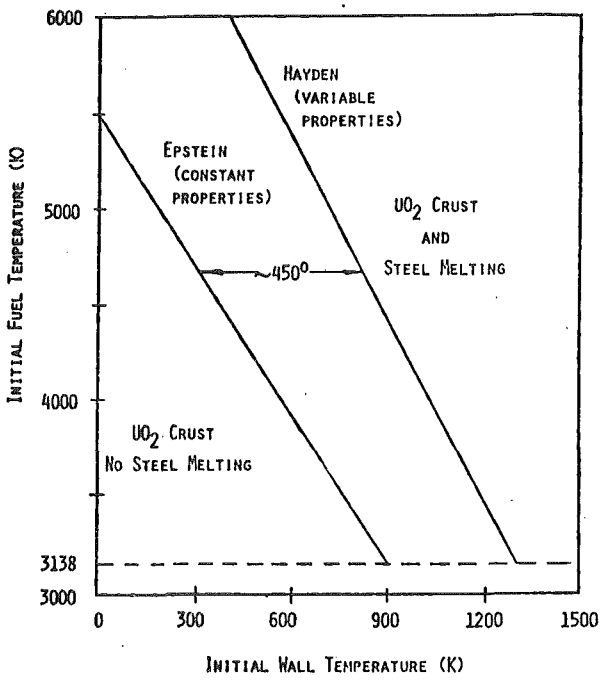

Fig. II.2.2.1 Initial Temperature Map for Initially Molten UO_2 Contacting Initially Solid Stainless Steel. Above Figure from /18/, below from /23/

Concerning the problem of blockage formation one would expect crust formation only in flat geometry or with flow in pipes (concave geometry), a situation which is also met in nature as lava flow in a volcano channel. Experiments however suggest that fuel crust formation should not be expected in real bundle geometry under accident conditions /22/.

Based on experimental information from uranium thermite tests, several analytical models have been derived which could at least give some guidance in interpreting the results /24, 25/ but did not really match the actually observed penetration distances.

o Bulk Freezing Model

This model assumes that because of turbulence within the flowing fuel no stable crust is formed at the wall of the channel. Freezing of fuel occurs when the bulk temperature of the leading edge of molten fuel reaches the freezing temperature. Plugging of a channel is assumed to be complete when the latent heat of fusion is removed from the leading edge of the flow by further turbulent heat loss to the wall

$$X_{PB} = \frac{1}{2}\frac{D}{f}\left[\frac{L_f/C_f + (T_f - T_{f,mp})}{T_f - T_s}\right]$$

The model applies for high fuel velocities and hot steel wall temperatures. Order of magnitude of $X_{PB} \sim$ cm.

o Conduction Freezing Model

The model assumes the formation of a solid fuel crust on a solid/liquid steel layer. Transient freezing is governed by heat conduction through the growing fuel layer. Penetration length is limited by the crust growth

$$X_{PC} = \frac{D^2 v}{16\lambda_f^2 \beta_f}$$

The model applies for low fuel velocity, rel. cold steel walls, tube flows. Order of magnitude of $X_{PC} \sim$ m.

o Ablation Induced Freezing Model

This model takes into account both heat conduction and turbulent heat transfer in the melt and mechanical stability of fuel crusts. Behind the leading fuel front the originally formed crust breaks up and the cold molten steel mixes with the flowing fuel and causes freezing in a bulk manner. Bulk freezing occurs when the fuel crust growth process is transformed to a steel ablation process

$$X_{PA} = X_{PB}(T_{s,mp}) \cdot \left[1 + \frac{T_{f,mp} - T_{s,mp}}{L_s/C_s + T_{s,mp} - T_s} \right]^{-1}$$

The model applies to high fuel velocities and hot steel temperatures. Order of magnitude of $X_{PA} \sim$ cm; $X_{PA} < X_{PB}$.

More recent reactor material fuel freezing experiments by Spencer et al. /27, 22/ with uranium thermite ejected with 3470 K and with pressures of 30 - 60 bar into a 7 - 37 pin test section show penetration distances that are shorter than predicted by a crust-growth model but farther than predicted by a bulk freezing model. Post-test examinations have shown no evidence of stable crust formation on the outside of cladding but have revealed extensive cladding melting and intermixing with fuel. To reach the above pressure levels during initiation or pretransition phase nuclear power bursts with some energetics potential must have occurred.

The tests have shown an apparent effect of fuel mass and fuel/steel clad temperature on the leading edge penetration distance. High injected fuel masses per pin of test section and high clad temperatures (T_s > 870 K) lead to penetration distances of 1.2 m. For lower temperatures (570 K) penetrations of 30 - 40 cm are obtained. Lower fuel masses per pin give penetration lengths of 30 - 40 cm for T_s > 870 K. For the first set of conditions the plug leading edge was composed of dense frozen steel, for the other conditions both UO_2 and steel are present at the leading edge. The results have been interpreted on the basis of a model depicted in /22/: Formation of an initial UO_2 plug due to bulk freezing of UO_2 at the front of the injected fluid mass - meltout of restraining steel clad structure by heat conduction from the blockage - extended motion of a mixture of melted steel and solidified UO_2 with the ultimate incremental penetration determined by conduction controlled freezing of melted steel.

The conclusion that can be drawn from the experimental information is that the mode of molten fuel freezing is dependent upon wall melting conditions. With no steel wall melting the conduction model may serve as guidance for estimating penetration distances. Thus these models may be used for assessing fuel penetration between hexcans, tube flow in control/dummy elements and in the PAHR phase. Rather long penetration paths can be expected. Fuel particles, voids etc. in the flowing fuel reduce the penetra-

BULK FREEZING MODEL

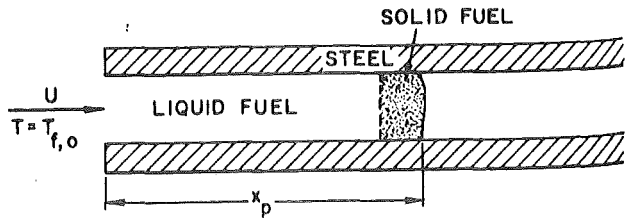

CONDUCTION FREEZING MODEL

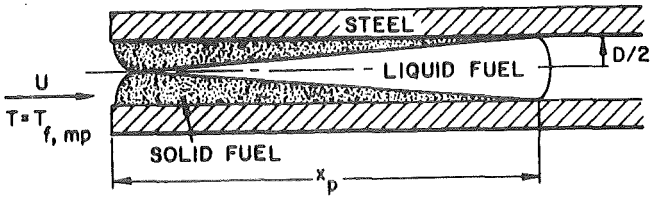

ABLATION INDUCED FREEZING MODEL

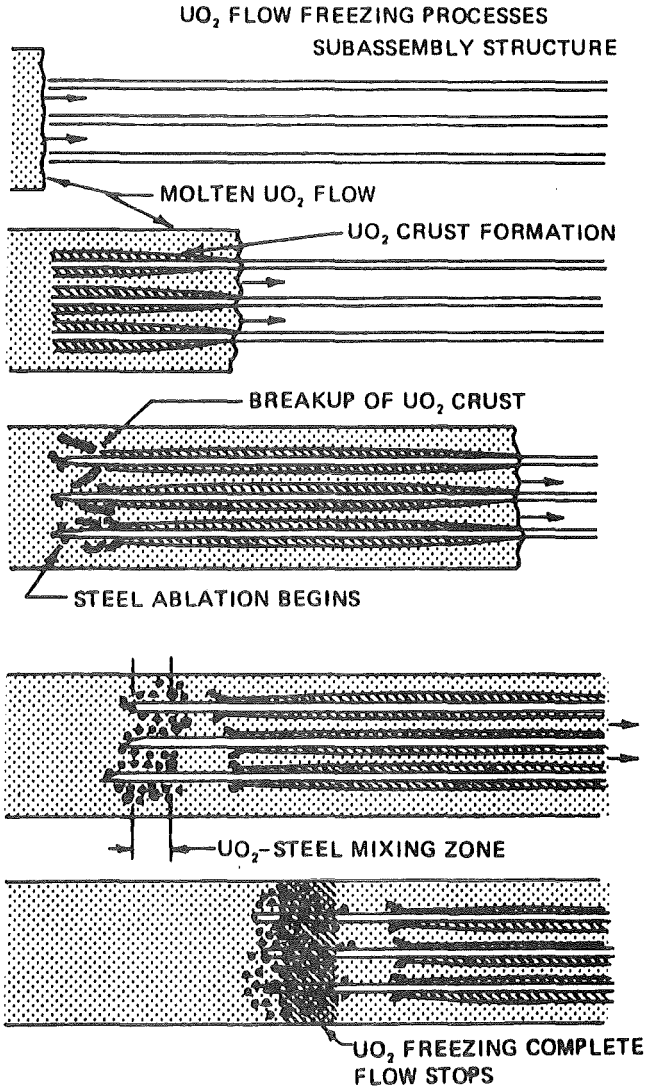

Fig. II.2.2.2 Fuel Freezing Models (bulk freezing, conduction freezing, ablation induced freezing) /19/

tion distances /26/. With wall melting fuel penetration and freezing depend on the stability of a frozen crust. In real bundle geometry and under transient conditions fuel crusts obviously are not formed. Thus the penetration distances of molten reactor material should be expected in the order of magnitude of some 10 cms under the conditions of a non-energetic initiation/pretransition phase.

II.3 FLOW REGIMES IN BOILING POOLS

If continuous fuel removal from the core does not lead to permanent nuclear shutdown during the pretransition phase, the continuing core disruption eventually results in a pool of molten and vaporized materials. Initially the pools contained with their individual subassembly ducts behave rather incoherently. As the duct walls melt away, corewide coherent movements become possible. Unless most of the original fuel inventory (40 - 50 %) has been removed from the core the fuel might reconfigure into a critical mass (Chap. II.1) and cause a neutronic power burst. Recriticality can be prevented if the fuel does not compact into a denser configuration but is in a dispersed two phase state. As mentioned before due to the vicinity of the fuel melting point and the steel boiling point the vapour source steel has the potential to disperse the heat source fuel, if both components are mixed.

Dealing with dispersed pools means dealing with flow regimes. Important items for assessing the impact of the flow regime on pool behaviour are (1) the relationship of the void fraction which determines the average "boilup" of the pool and the slip velocity between vapour and liquid, (flow regimes with higher slip velocities (e.g. droplet dispersed) are less capable of carrying the liquid and can be classified as less dispersive), (2) effects of heat transfer to the pool boundaries (Chap. II.4) and (3) effects of boiling pool dynamics (Chap. II.1).

Experimental information on internally heated fluids and flow regimes has been gained mainly in open structure. In addition most of the information comes from quasistatic pools whereas there are only few experiments actually dealing with the dynamic behaviour of pools such as boilup, collapse, density oscillations etc. For the purpose of evaluating boiling flow re-

gimes and predicting the extent of fuel dispersal Fauske /28/ has developed transition criteria and approximate boundaries separting the prevailing flow regimes for a LMFBR fuel/steel pool situation. These criteria had been developed from early experimental data from systems characterized by surface gas/liquid into liquid injection of Kutateladze /29/. By starting with the Kutateladze stability criterion /29/ (stability of the overall flow structure is determined by the stability of the elements of the phases comprising it - droplets, bubbles etc.), which relates dynamic forces to surface tension forces, a dimensionless stability parameter K can be derived

$$K = \frac{j\sqrt{\rho c}}{\sqrt[4]{g\sigma(\rho_H - \rho_L)}}$$

The superficial velocity j in an internally heated fluid can be determined according to

$$j = \frac{Q(1-\bar{\alpha})\,X}{\rho_L\, h_{fg}}$$

The parameter K has to be obtained from experiment. On the basis of this information Fauske /28/ suggested three flow regimes in volume heated boiling pools, bubbly, churn turbulent and droplet dispersed flow regime - in the order of increasing superficial velocity - and constructed a flow regime map for different power levels in the transition phase pool. He argued /28/ that even at decay power levels the fuel/steel mixture in the pool would exist as a dispersed, fluidized droplet flow regime and neutronically critical configurations should not exist above 1 % of nominal reactor power.

However the application of the Kutateladze criterion to volumetrically heated pool experiments showed significant deviations from the original values though the basic approach to define flow regimes was confirmed. Both the churn turbulent flow regime persisted at much higher superficial vapor velocities and the transition between flow regimes occurred over a range of superficial velocities rather than a unique value. Transition to the droplet dispersed regime occurred at much higher power levels as origi-

nally stated. In Tab. II.3.1 the original Fauske values /28/ are compared with those of recent experiments and in Fig. II.3.1 the implication on the flow regimes in a boiling fuel/steel pool (open pool) is displayed.

Nature of Process	K /28/	K /17/	K /30/	K /31/
Breakdown of bubbly flow $\rho_c = \rho_H$	0.3	0.3-0.6	-	-
Breakdown of churn turbulent flow - drop fluidization of a heavier fluid by a lighter fluid $\rho_c = \rho_L$	0.14	-	1.4	0.42

Tab. II.3.1 Values of the Stability Parameter K

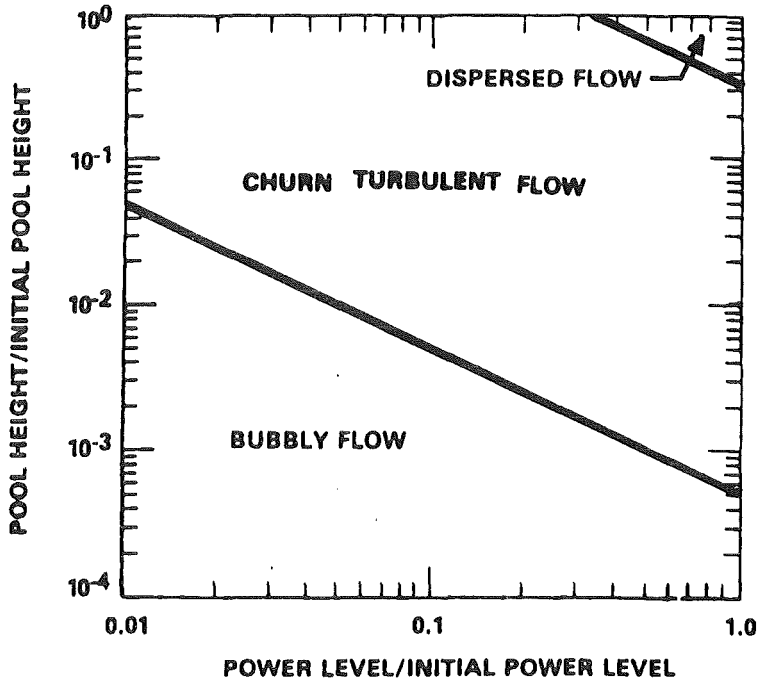

Fig. II.3.1 Flow Regimes in a Boiling Fuel/Steel Pool

Koontz /17/ performed experiments in both one and two component boiling pools. Thus accounting for the fact that in a nuclear boiling pool the heat and the vapor source are not identical. For his experiments he used both joule and microwave heating and his simulant fluids were hexane (heptane) in combination with water. For the one component boiling test he obtained a transition constant K for bubbly/churn of $\sim$ 0.6 whereas for 2-component boiling it is about 0.3. Also "dynamic" experiments where cutoff of hexane injection and boiloff with subsequent pool collapse or rapid injection of cold heptane with ultimate pool collapse are reported simulating processes that may occur in fuel/steel pools as discussed in Chap. II.1. Pool collapse rates were rather slow however further studies are obviously needed /32/.

Recent experiments by Greene et al. /33/ were performed in an open boiling system in which joule heating was used to generate volumetric boiling. Both the bubbly and the churn turbulent flow regime have been observed. The average void fraction $\bar{\alpha}$ was measured and compared to the dimensionless superficial vapor velocity $j_{g\infty}/U_\infty$ (U_∞ single bubble rise velocity). The bubbly flow regime persisted for a value of $j_{g\infty}/U_\infty$ up to unity. The pool exhibited a stratified state with a boiling region over an essential non-boiling single phase region which depth decreased with increase of volumetric vapor source. The maximum average void fraction observed was in the range of 0.55 - 0.60. The void fraction was found to vary sensitively with volumetric power. Flow regime transition from bubbly to churn turbulent flow was observed to occur at $j_{g\infty}/U_\infty \sim 1.0$. The flow regime transition was accompanied by a marked collapse in average pool void fraction from 0.55 - 0.60 to 0.40 by large scale bubble agglomeration. The pool hydrodynamics appeared to behave in a 3-dim. fashion. The void fraction appeared somewhat insensitive to increase in pool power for $1.0 < j_{g\infty}/U_\infty < 2.0$.

Besides these experiments /17, 33, 34/ which are characterized by relatively low pool average void fraction with the bubbly and churn turbulent flow regime prevailing flow regimes have also been reported with very high void fractions of 70 - 90 % /34, 35/ in a stable foam regime. This foam flow regime seems to exist due to system contaminants as particulate and chemical impurities. Fig. II.3.2 gives a review of the various pool average void fraction measurements.

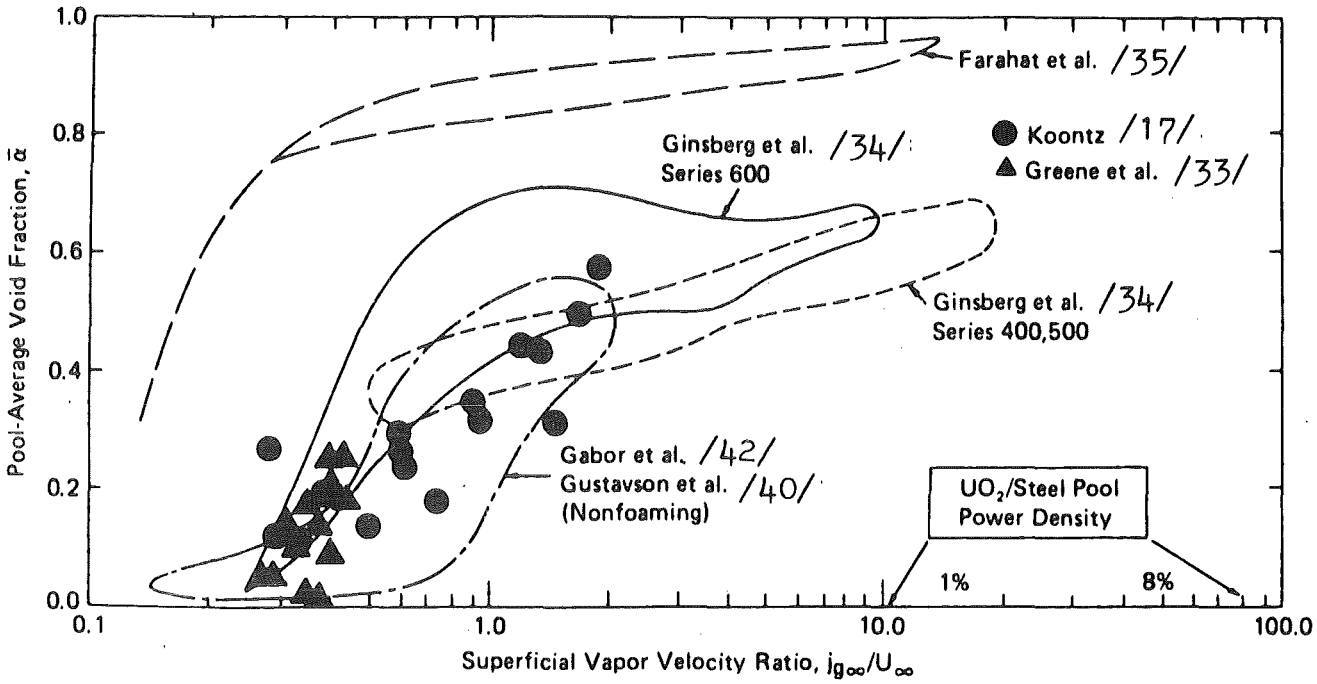

Fig. II.3.2 Pool Average Void Fraction Measurements /34/

As could be demonstrated by Farahat /35/ boilup and core material dispersion can also be expected in a bottled up core situation. If the bottled up system would be adiabatically heated up by fission/decay heat the vapor velocity would rapidly drop leading to compaction of the pool. However, upward heat sinks, where the vapor from the pool can condense, could maintain boilup (Chap. II.4).

Due to Fig. II.3.1 the dispersed flow regime is not to be expected at decay heat levels both in open and bottled up pools but only under nominal power or power pulse conditions. In a bottled up pool situation the flow regime transition lines of Fig. II.3.1 are dependent on the vapor condensation capability of the structures above the pool. In the case of an idealized adiabatic closed pool the power densities e.g. for reaching the dispersal limit (churn turbulent → dispersed flow) may be two orders of magnitude higher /49/ than for an open pool. This is because in an adiabatic pool most of the energy generated is used to increase the sensible heat of the liquid and only a small fraction of the available energy is used to generate vapor.

II.4 HEAT TRANSFER FROM INTERNALLY HEATED POOLS

The stability of a boiling pool strongly depends on its heat transfer rate to the surroundings. If the heat transfer rate from a bottled boiling pool is less than the heat generation rate the pressure inside the pool will increase, if the heat transfer rate is too high the pool might collapse. In the case of an open pool system the dominant mode of heat transfer is the transport of steel vapor which maintains the pool in a boiling state, and its loss from the pool. Using the relationship between the superficial velocity and internal heat generation and the results of e.g /33/ (Chap. II.3) it can be shown that for pool boilup only a small fraction of pool power (< 1 % nominal) is needed for boilup.

In a bottled up pool a similar boilup could be maintained if adequate condensing surfaces exist above the pool /35/. In constrast to the open system in the bottled up pool a closed loop of mass flow is established with refluxing of the condensed fuel/steel mixture on the sidewalls. The boilup behaviour of a bottled up pool is determined by the ratio of the condensation (upper structure) to the noncondensation heat losses (bottom, lateral boundary structure). The noncondensation heat losses tend to decrease pool temperature without contributing condensing capacity for promoting vapor generation.

The phenomenon of fuel crust formation (see Chap. II.2) plays also an important role in assessing the boilup and heat transfer in boiling fuel/steel pools. The formation of a fuel crust at the pool boundary can strongly reduce the noncondensation heat losses. The presence of an isolating crust that forms on contact of hot fuel with cold steel could reduce the heat transfer driving temperature between the bulk boiling pool and the wall by an order of magnitude (with crust $\Delta T \sim T_{pool} - T_{Solid}^{Fuel} \simeq$ 100 K without crust $\Delta T \sim T_{pool} - T_{melt}^{steel} \simeq$ 1500). The crust (thickness δ) is attributed a self-regulating behaviour due to $\delta_{max} = \sqrt{2K(T_{pool} - T_s)/Q}$ having small/thick crusts for high/low internal heat generation. Experiments and theoretical evaluations /18-21/ back the assumption of a solid crust at the pool boundaries, however mechanical and thermal crust break up under violent pool conditions (structure buckling etc.) /27/ cannot be excluded.

Theoretical stability limits (boilup versus collapse) for bottled up UO_2 pools for various sizes have been given in /37/. The mechanisms of heat removal to the noncondensing surfaces (sides + bottom) of the pool are by conduction and convection. The heat flux to the top boundary is due to condensation of the rising vapor. The two limits for pool boilup are given by (a) the superficial vapor velocity required to maintain a steady pool void fraction and boilup and (b) the maximum possible rate of condensation on the underside of the top surface. Over a wide range of heat generation rates stable boiling conditions could be demonstrated. The heat flux distribution in the pool showed that the sideward heat flux was the principal heat removal mechanism with the upward/downward heat fluxes being of the same order of magnitude.

Though it could be demonstrated experimentally /35/ and theoretically /36,37,38/ that also under bottled up core situations there exists a large potential for pool boilup imbalances between condensation heat losses and heat losses to the structure with the power production etc. can directly lead to dynamic compaction processes as discussed (Chap. II.1).

Experimental information on boundary heat transfer from volume-boiling pools (simulant fluid: water-electrolyte) has been gained mainly by the work performed at Brookhaven /33,39,40/ and Argonne National Laboratory /41,42/. In Brookhaven the first attempts were made to determine the spatial variations in local heat transfer coefficients and local void fractions in such boiling pools. Such local quantities are important since the local heat transfer coefficient may be significantly higher than the average values and thus the higher local rates will determine the melting attack on solid structure.

In /40/ it was proposed that the boundary heat transfer from volume heated boiling pools was a mixed free and forced convection type heat transfer phenomenon in which the effects were superimposable. Greene et al. /39/, however, argued that the phenomenon was driven simply by the buoyancy induced by the two phase density differences between the wall and the bulk mixture. Heat transfer from a volumetrically boiling pool to a vertical surface exhibits a behavior like a single phase natural convection boundary layer, enhanced by the flow of net liquid recirculation due to upward vapor drag through the central liquid and downward along the walls (Fig. II.4.1).

Single phase natural convection boundary layer theory coupled with the buoyancy effect of the two phase vapor distribution in the bulk liquid was used to correlate the Nusselt number to a modified Rayleigh number which contains the single phase buoyancy effect and the effect due to void distribution.

$$Nu(x,\alpha,\theta) = 0.76\left[Gr^*(x,\alpha,\theta)\cdot Pr\right]^{0.25}$$

$$Gr^*(x,\alpha,\theta) = \frac{g\cos\theta\left[(\rho_w - \rho_{\ell\infty}) + \alpha\rho_{\ell\infty}\right]\rho_f X^3}{\mu_f^2}$$

If $\alpha\rho_{\ell\infty} >> \rho_w - \rho_{\ell\infty}$ this may be reduced to

$$Gr^*(x,\alpha,\theta) = \frac{g\cos\theta\alpha x^3}{\nu_f^2}$$

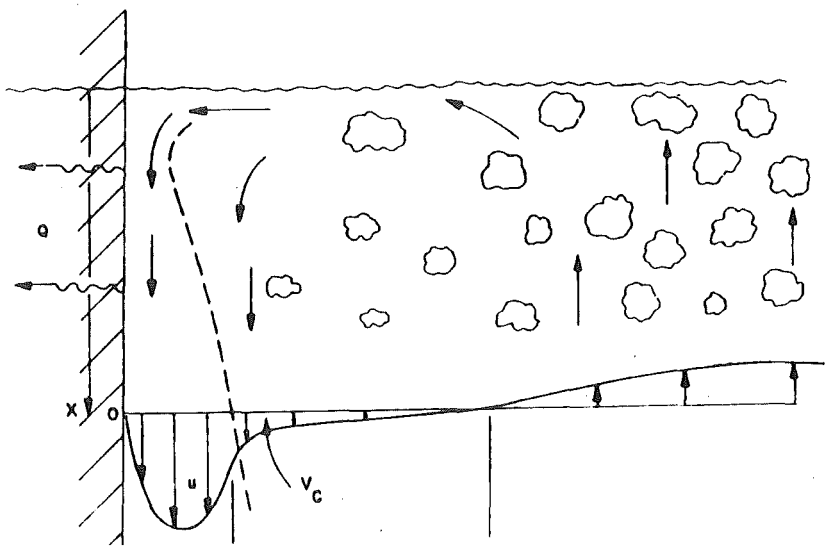

Fig. II.4.1 Natural Convection to a Vertical Surface Adjacent to a Volume Heated Boiling Pool /33/

Experimental information /33/ confirms the boundary heat transfer from volume boiling pools in the bubbly flow regime to behave similar to natural convection type boundary layer heat transfer though local heat transfer coefficients are higher as given by the above correlation. The greatest heat transfer was near the pool surface. The local heat transfer coefficients developed on the basis of the measurements for the bubbly flow regime are given in /48/:

$$Nu(x) = (1.41 \pm 0.240)\ Ra^{*0.25} \qquad Ra^* < 7.36 \cdot 10^{11}$$

$$Nu(x) = (0.0234 \pm 0.002)\ Ra^{*0.40} \qquad Ra^* > 7.36 \cdot 10^{11}$$

Correlation of average heat transfer based on the average void fraction indicates laminar flow behavior up to Rayleigh number of $1.865 \cdot 10^{11}$. For higher Ra^x-Numbers the data behave similar to turbulent natural convection

$$\overline{Nu} \simeq 1.54\ Ra^x(L, \bar{\alpha}, \theta)^{0.25} \qquad Ra^x < 1.865 \cdot 10^{11}$$

$$\overline{Nu} \simeq 0.0314\ Ra^x(L, \bar{\alpha}, \theta)^{0.40} \qquad Ra^x > 1.865 \cdot 10^{11}$$

For the churn turbulent flow regime the data deviated sharply from the above behavior. The average heat transfer was approx. 0.6 Watt/cm²°C (bubbly $\sim$ 0.4). Large temporal fluctuations in the wall temperature were observed indicating local destruction and renewal of wall boundary layer and leading to the increased boundary heat transfer coefficient. The maximum local lateral heat transfer coefficient was observed to be in the range 1.0 - 1.3 Watt/cm²°C (bubbly $\sim$ 0.8).

In a recent interpretation /47/ the heat transfer data of Gabor /42/ and Greene /39/ are correlated on the model assumption that due to the density difference caused by volume boiling and by thermal expansion between the bulk fluid and that near the wall the lighter fluid and vapor bubbles cause movement of the bulk fluid in the upward direction and refluxing at the pool boundaries. At the wall the boundary layer that may be laminar in its initial lengths changes to turbulent. In the laminar case the natural convection is characterized by $Gr = \left[\gamma(T_{bulk} - T_{wall}) + 3\alpha\right] g\cos\theta x^3/\nu^2$. The heat transfer law derived for the turbulent flow is:

$$Nu = 0.16\ Ra^{1/3}\left[1 + (0.492/Pr)^{9/16}\right]^{-16/27}$$

The downward heat flux can be assessed on the basis of a correlation of the experimental data from Baker /37/ where the conduction heat flux across a stable heat layer of heat generating liquid is combined with a correction term f(j) which accounts for the turbulence caused by the bubble departure from the layer.

$$q_d = \left[K(T_{sat} - T_{mp})Q\right]^{1/2}(1-\bar{\alpha})f(j)$$

$$f(j) = \exp(0.588 + 0.106j - 0.00227j^2) \qquad j < 24.34 \text{ cm/sec}$$

$$f(j) = 6.206 \qquad j \geq 24.34 \text{ cm/sec}$$

The upward heat flux in a bottled up pool can be estimated by the amount of vapor reaching the underside of the top blockage and can be condensed there. The maximum condensation rate is governed by the boundary layer that will develop from the condensation as well as the steel melt (steel droplets drip down) on the underside of the upper surface /37,46/.

$$q_u = 0.69(\tilde{Ra})^{0.2}K(T_{sat} - T_{mp})/(\sigma/\rho_\ell g)^{1/2}$$

$$\tilde{Ra} = \frac{g(\rho_\ell - \rho_v)h_{fg}}{K\cdot\nu\cdot(T_{sat} - T_{mp})}\cdot\left(\frac{\sigma}{g\rho_\ell}\right)^{3/2}\left(\frac{L + c_s(T_{mp} - T_o)}{L + h_{fg} + c_s(T_{mp} - T_o)}\right)$$

The presence of noncondensible gases can reduce the condensation rate by an order of magnitude.

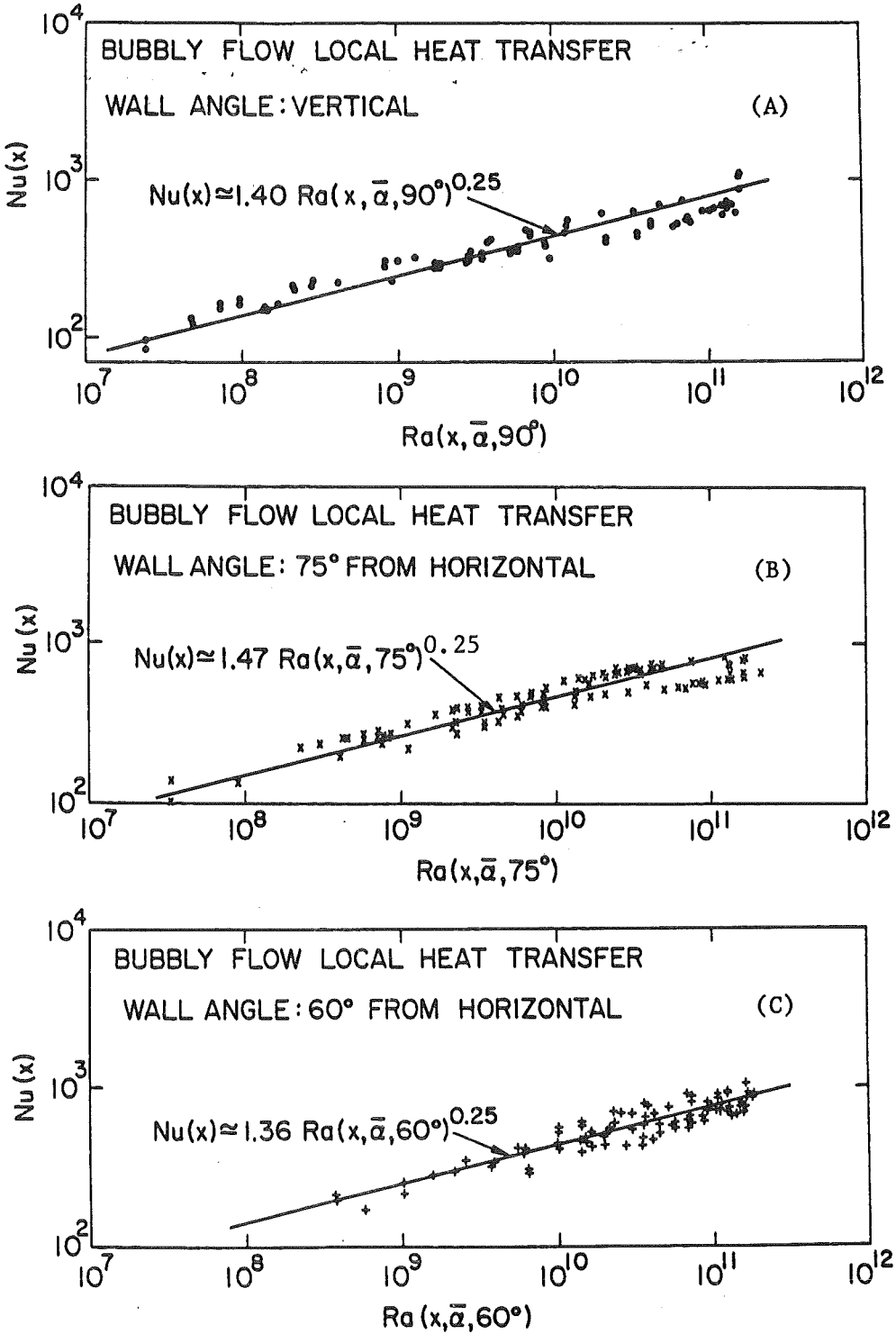

Fig. II.4.2 Correlation of Local Heat Transfer Data from Volume-Boiling Pools in Bubbly Flow : $Ra^* \leq 2.10^{11}$ (from /48/)

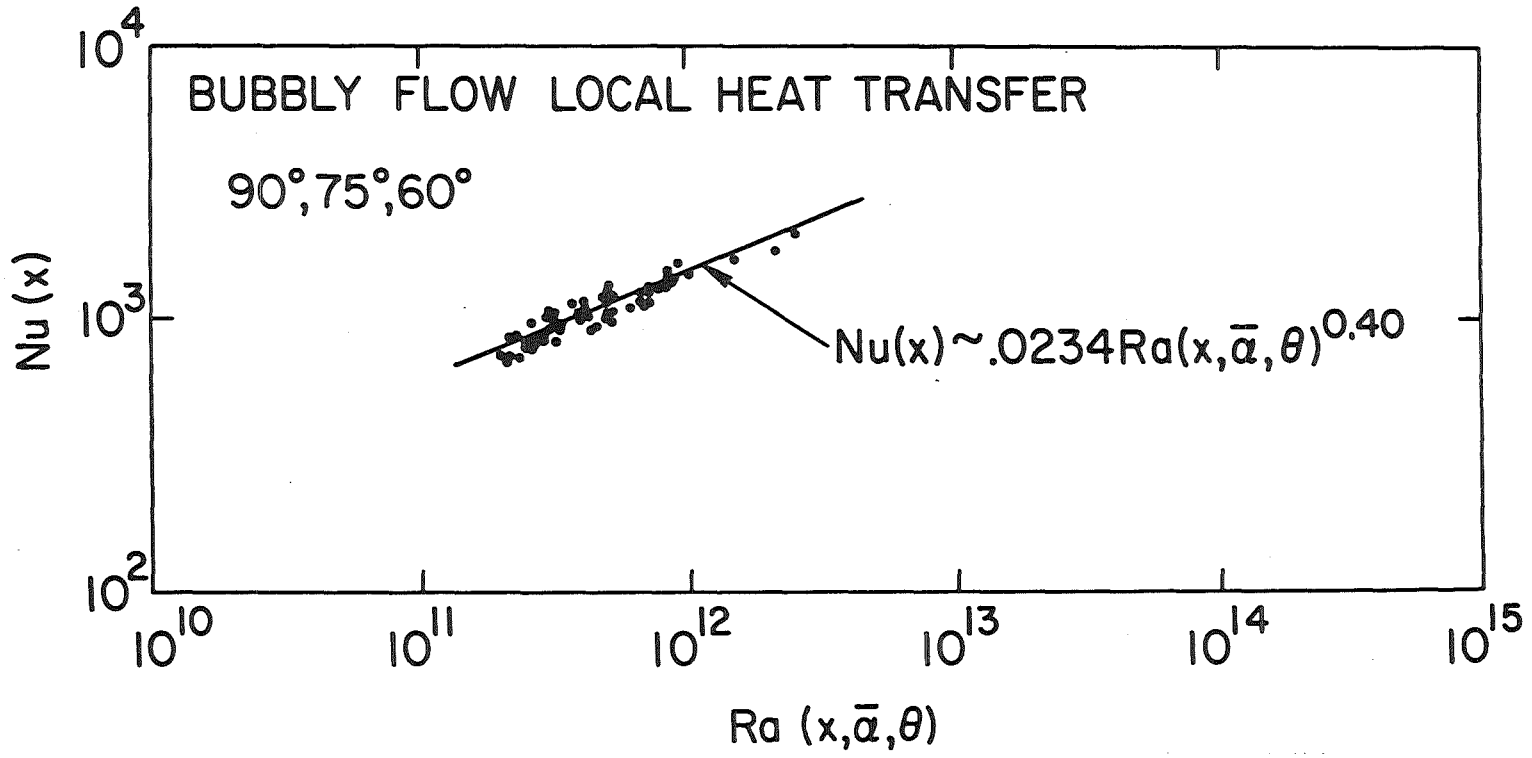

Fig. II.4.3 Correlation of Local Heat Transfer Data from Volume-Boiling Pools in Bubbly Flow : $Ra^{*} > 2.10^{11}$
(from /48/)

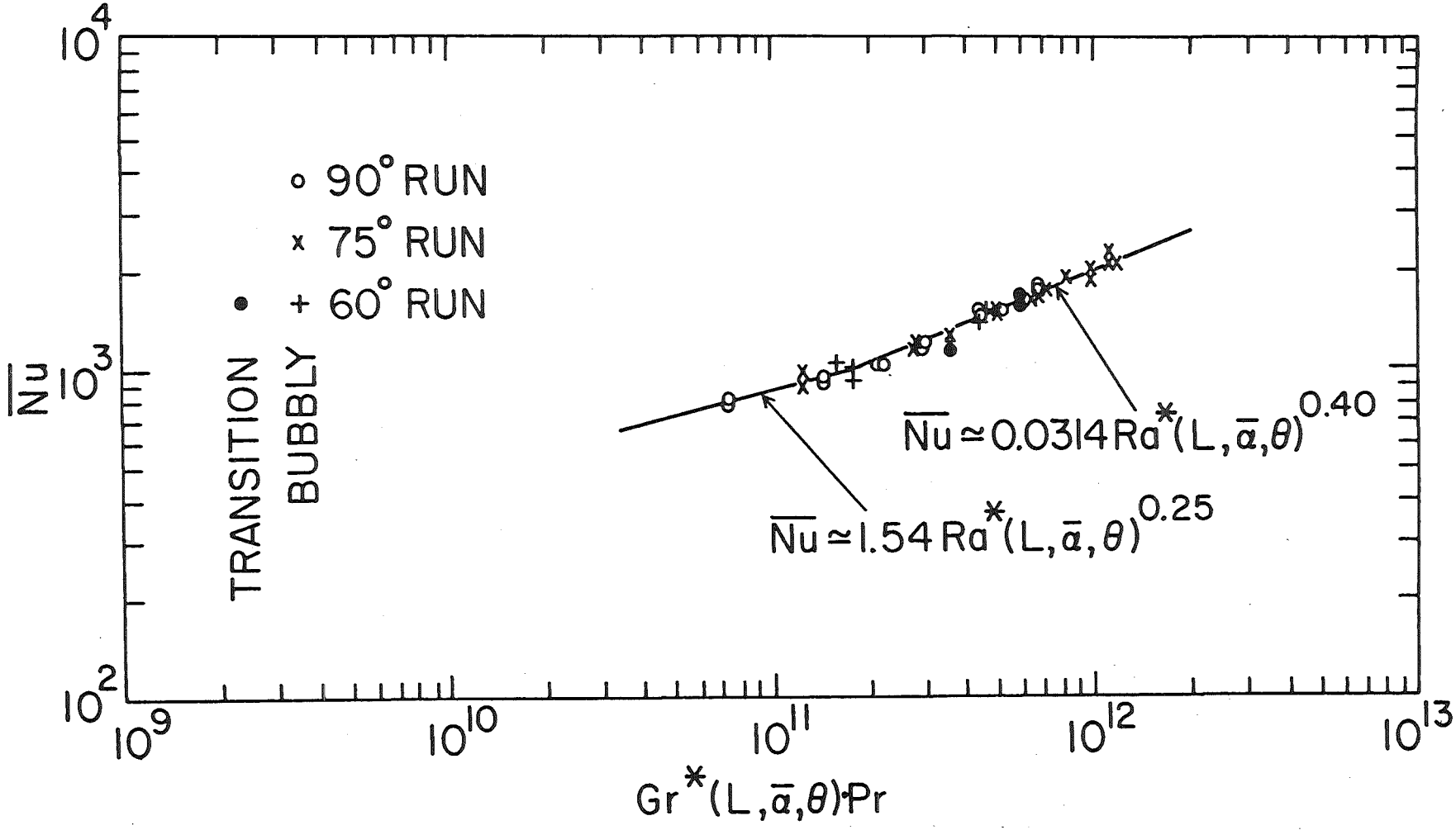

Fig. II.4.4 Lateral Boundary Heat Transfer Correlations from Volume-Boiling Pools /33/

AUTHOR	WALL ANGLE	LOCAL OR AVERAGE HEAT TRANSFER	LAMINAR OR TURBULENT	BEST FIT CORRELATION	STANDARD DEVIATION	RANGE OF RAYLEIGH NUMBER
Gustavson, et al.[12]	Vertical	Local	Laminar	$Nu(x) = .78\ Ra^*_{(x,\bar{\alpha})}{}^{0.25}$	$\pm$ .35	$Ra^* < 10^{12}$
		Local	Laminar	$Nu(x) = .76\ Ra^*_{(x,\alpha)}{}^{0.25}$	$\pm$ .56	$Ra^* < 10^{12}$
		Average	Laminar	$\overline{Nu} = 1.07\ Ra^*_{(L,\bar{\alpha})}{}^{0.25}$	$\pm$ .30	$Ra^* < 2 \times 10^{12}$
Gabor, et al.[11]	Vertical	Average	Laminar	$\overline{Nu} = 1.58\ Ra^*_{(L,\bar{\alpha})}{}^{0.25}$	$\pm$ .33	$Ra^* < 2 \times 10^{12}$
		Average	Laminar	$\overline{Nu} = 1.42\ Ra^*_{(L,\bar{\alpha})}{}^{0.25}$	$\pm$ .25	$Ra^* < 10^{11}$
		Average	Turbulent	$\overline{Nu} = .0309\ Ra^*_{(L,\bar{\alpha})}{}^{0.40}$	$\pm$ .0058	$Ra^* > 10^{11}$
Present Work	90°, 75° 60°	Average	Laminar	$\overline{Nu} = 1.54\ Ra^*_{(L,\bar{\alpha},\theta)}{}^{0.25}$	$\pm$ .08	$Ra^* < 1.865 \times 10^{11}$
		Average	Turbulent	$\overline{Nu} = .0314\ Ra^*_{(L,\bar{\alpha},\theta)}{}^{0.40}$	$\pm$ .0016	$Ra^* > 1.865 \times 10^{11}$

Tab. II.4.1 Summary of Local and Average Correlations for Heat Transfer from Volume Boiling Pools /33/

III. MECHANISTIC ANALYSIS OF THE TRANSITION PHASE

Analysis of the transition phase mainly deals with the question if fuel redistribution processes could result in neutronically critical material configurations. If superprompt criticality is achieved an energetic nuclear power excursion with the build-up of fuel vapor pressures could mechanically disassemble the already disrupted core configuration and could lead to mechanical loadings of the vessel structures.

The recriticality potential, the recriticality event itself and the resulting nuclear power burst are usually assessed on the basis of complex computer simulations, on the basis of fundamental physical principles ("general behavior principles" /43/) and the available experimental information. Most of the recriticality analyses up to 1979 (e.g. /44/) were based on the investigation of idealized "model cases" which cover the most important forms of recriticality and give - by a consequent pessimistic modelling - bounds for the energetics of recriticality events. The various conceivable modes of recriticality (Chap. II.1.2) were investigated using codes like SAS3D /4/, KADIS /6/ and simple unpublished codes/models based on phenomenological understanding /7/. The energetics that have to be expected for SNR300 range up to about 100 MJ mechanical energy (determined by isentropic expansion of the hot fuel vapor/liquid mixture to the stretched covergas volume of SNR300).

In 1979 Bohl /16/ presented the first fully mechanistic calculation of the transition phase starting from a SAS3D calculation of the initiation phase and following up the further core disruption with the SIMMER-II code /5/. With the SIMMER-II code the highly nonlinear feedback between neutronics and thermo-fluiddynamics can be adequately taken into account. From the calculations with SIMMER-II the conclusion was drawn that a bottled up pool situation will eventually lead to pool collapse and that stable pool boilup without recriticality /43/ is improbable.

The importance and advantage of the mechanistic analyses is obvious, as arbitrary and overly pessimistic assumptions or postulates for the assessment of the recriticality events can be largely discarded. An example for a mechanistic calculation of the pre- and -transition phase with SIMMER-II for a SNR-type reactor is given below.

The initial conditions for the SIMMER-II analysis were established by calculations of the initiation phase of the accident with the SAS3D code. Axial fuel expansion and early fuel dispersion make the course of the accident rather mild during initiation phase with a primary power excursion of only about 30 times the nominal power level. However, this first power transients makes the core material mobile and activates further material redistribution processes. First material compaction processes due to nuclear power reduction after the first burst and loss of vapor pressure sources leads to mild power excursions of about 20 times nominal power. As the hexcan structure is mainly intact material motions are rather incoherent and reactivity ramp rate insertions are low.

Steel melting of the hexcan structure and quenching of dispersive vapor pressures generate a wide-spread fuel collapse and a mild prompt critical burst (290 times nominal power). Melting of the hexcan structure leads to an entry of reactivity reducing blanket material into the core. This causes both a drop in reactivity (- 20 $ at the end of the SIMMER calculation) by the fuel dilution but also to a quenching of the core fuel by the cold blanket material. The SIMMER calculation is stopped at this time (terminated in the pretransition phase) as now processes which could not be adequately handled by SIMMER will become dominant (remelting by decay heat, fuel/steel separation processes etc.) and no further "energetic" event is to be expected due to blanket mix-in. The course of the accident is displayed in Fig. III.1 by means of the nuclear power trace. The model parameters of the calculation have been chosen in such a way that freezing and blockage formation in the axial blanket structure prevents early continuous material discharge from the core and attainment of subcriticality. If no blanket material could enter the core region after hexcan melting eventually a whole core pool would be built-up. The power bursts calculated under these conditions range up to 100 MJ mechanical energy (isentropic fuel vapor expansion to cover gas volume).

Under specific SNR-300 conditions (axial blanket $\sim$ 40 cm, fission gas plenum below the core, high pitch/diameter ratio of fuel pins) however substantial material discharge is to be expected during the pretransition phase. Blanket pellet melt and drop-in after hexcan melting has the potential to reduce nuclear criticality to levels far away from prompt criticality. Only in the case of no discharge and no blanket material entry

energetic scenarios have to be envisaged. The bottled up core situation and related scenarios are estimated as pessimistic accident paths with lower probability.

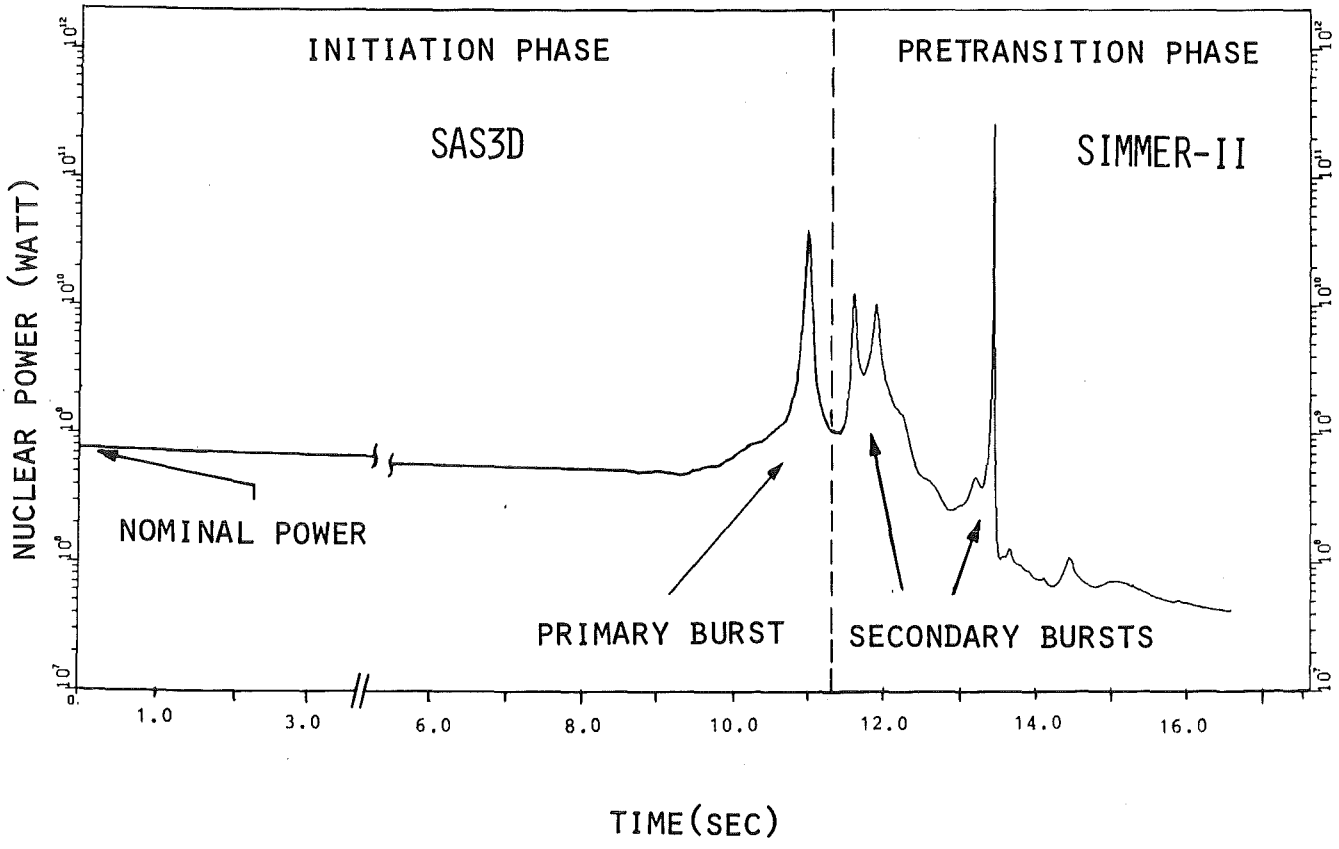

Fig. III.1 Nuclear Power Trace of Mechanistic SAS3D/SIMMER-II Calculation

IV. CONCLUSIONS AND FINAL REMARKS

In the last years considerable progress has been made in understanding phenomena and processes pertaining to the pre- and transition phase.

Experimental information about fuel freezing leads to the conclusion that the built-up of a totally bottled pool within the core region is rather unlikely for SNR-typical conditions. The partly open blanket structures allow for fuel transport out of the core region and still available hexcanstructures introduce enough incoherence in fuel motion to prevent energetic recriticalities. In addition drop-in of blanket material will effectively dilute the core fuel. In this way it is expected that a bottled up pool situation, with a potential for energetic recriticalities, could be avoided. Thus the accident may directly enter the PAHR-phase after pretransition phase. Therefore blockage formation in colder structures and related phenomena is a key phenomenon which should be further investigated. If material discharge could be conclusively demonstrated under pretransition phase conditions one would gain much relief in the recriticality question.

A conclusion that can be drawn from the mechanistic SIMMER-II transition phase analyses is, that the possibility of recriticalities during accident situations with large amounts of undiluted molten material confined in a bottled up pool configuration cannot be ruled out. However, also under these conditions incoherence effects limit reactivity insertion rates. It should be emphasized: If a transition phase with a high inventory, undiluted pool is reached, the behavior of this molten/boiling pool is the most important issue. Further experimental and theoretical efforts should deal with the transient behaviour of these pools (dispersal-compaction).

Better understanding of the above phenomena could help to reduce the numerous conservatisms in estimating the accident energetics and could lead to a more realistic assessment of the HCDA.

Acknowledgements

I would like to thank Dr. R. Fröhlich for critical discussions and comments and Mrs. G. Bunz for carefully typing this paper.

V. REFERENCES

/1/ Fröhlich, R. et al.:
Safety Related Physics Activities in the DEBENE-FBR Project
KfK 3082 (1980)

/2/ Jackson, J. F. et al.:
Trends in LMFBR Hypothetical Accident Analysis
Proc. ANS Fast Reactor Safety Conference, Beverly Hills, California
CONF-740401, pp. 1241 (1974)

/3/ Royl, P. et al.:
Untersuchungen zu Kühlmitteldurchsatzstörfällen im abgebrannten Mark 1A Kern des Kernkraftwerks Kalkar
KfK 2845 (1978)

/4/ Cahalen, J.:
A Preliminary User's Guide to Version 1.0 of the SAS3D LMFBR Accident Analysis Computer Code SR 239831
ANL, July 1977

/5/ Smith, L. L. et al.:
SIMMER-II: A Computer Program for LMFBR Disrupted Core Analysis
LA-7515-M (1978)

/6/ Schmuck, P. et al.:
KADIS - Ein Computerprogramm zur Analyse der Kernzerlegungsphase bei hypothetischen Störfällen in schnellen natriumgekühlten Brutreaktoren
KfK 2497 (1977)

/7/ Maschek, W. et al.:
Recriticality Considerations and Core Material Redistribution in the Reactor Vessel of SNR-300 as a Consequence of Loss of Flow Transients in the Mark 1A Core
Proc. Int. Meeting on Fast Reactor Safety Technology, Seattle 1979, pp. 721

/8/ Chawla, T. C. et al.:
Thermophysical Properties of Mixed Oxide Fuel and Stainless Steel Type 316 for Use in Transition Phase Analysis
Nucl. Eng. and Design 67, 57 (1981)

/9/ Boudreau, J. E. et al.:
On Autocatalysis During Fast Reactor Disassembly
Nucl. Sci. Eng. 51, 206 (1973)

/10/ Maschek, W. et al.:
Transition Phase and Recriticality Analyses for a SNR-Type Homogeneous Core with the SIMMER-II Code
Int. Topical Meeting on Liquid Metal Fast Breeder Reactor Safety and Related Design and Operational Aspects, Lyon, France 1982

/11/ Maschek, W.:
Einfluß der Vorläuferkonzentrationen auf die Energetik von prompt kritischen Leistungsexkursionen
KfK 2988 (1980)

/12/ Boudreau, J. E. et al.:
Recriticality Considerations in LMFBR Accidents Fast Reactor Safety Meeting, Beverly Hills 1974,
CONF-740401, pp. 1265

/13/ Henry, R. E. et al.:
Experiments on Pressure-Driven Fuel Compaction with Reactor Materials
Int. Meeting on Fast Reactor Safety and Related Physics,
Chicago 1976, CONF-761001, pp. 1735

/14/ Spencer, B. W. et al.:
Results of Recent Upper Plenum Injection Tests
Int. Meeting on Fast Reactor Safety Technology, Seattle 1979,
pp. 1735

/15/ Spencer, B. W.:
Private communication

/16/ Bohl, W. R.:
Some Recriticality Studies with SIMMER-II
Int. Meeting on Fast Reactor Safety Technology, Seattle 1979,
pp. 1415

/17/ Koontz, F. A.:
Volumetric Boiling - A Fundamental Study of the Phenomena Pertaining to LMFBR Safety
Thesis, Purdue University (1977)

/18/ Epstein, M.:
Heat Conduction in the UO_2 Cladding Composite Body with Simultaneous Solidification and Melting
Nucl. Sci. Eng. 51, 84 (1973)

/19/ Epstein, M. et al.:
Transient Freezing of a Flowing Ceramic Fuel in a Steel Channel
Nucl. Sci. Eng. 61, 310 (1976)

/20/ Epstein, M.:
Stability of a Submerged Frozen Crust
J. of Heat Transfer 99, 527 (1977)

/21/ Epstein, M. et al.:
Simultaneous Melting and Freezing in the Impingement Region of a Liquid Jet
ASME Winter Annual Meeting, San Francisco 1978

/22/ Sienicki, J. J. et al.:
An Extended Material Motion Model for Thermite Fuel Freezing Tests
Trans. ANS 38 391 (1981)

/23/ Hayden, N. K.:
An Analytical Model of Freezing Liquid Penetration in Tube Flow
Trans. ANS 39, 671 (1981)

/24/ Ostensen, R. W. et al.:
Fuel Flow and Freezing in the Upper Subassembly Structure Following an LMFBR Disassembly
Trans. ANS 18, 214 (1974)

/25/ Epstein, M. et al.:
Analytical and Experimental Studies of Transient Fuel Freezing
Int. Meeting Fast Reactor Safety and Related Physics, Chicago 1976
CONF-761001, pp. 1788

/26/ Greene, G. A.:
Fuel Relocation Studies
Quarterly Progress Report - Advanced Reactor Safety Research Division, BNL (1980)
BNL-NUREG-51297, pp. 107

/27/ Spencer, B. W. et al.:
Summary and Evaluation of Reactor Material Fuel Freezing Tests
Proc. Int. Meeting on Fast Reactor Safety Technology, Seattle 1979, pp. 1766

/28/ Fauske, H. K.:
Boiling Flow Regime Maps in LMFBR HCDA Analysis
Trans. ANS 22, 385 (1975)

/29/ Kutateladze, S. S.:
Elements of the Hydrodynamics of Gas-Liquid Systems
Fluid Mechanics - Soviet Research, No. 1, 38 (1972)

/30/ Leung, J. C. M. et al.:
Transition to Dispersed Flow in a Stagnant Pool with Gas Injection
Trans. ANS 38, 397 (1981)

/31/ Ginsberg, T.:
Gas Injection Simulations of Aspects of Boiling Pool Flow Dynamics and Comparison with Previous Volume Boiling Studies
Trans. ANS 39, 654 (1981)

/32/ Theofanous et al.:
Multiphase Transients with Coolant and Core Materials in LMFBR Core Disruptive Accident Energetics Evaluations
NUREG/CR-0224 (1978)

/33/ Greene et al.:
Heat Removal Characteristics of Volume Heated Boiling Pools with Inclined Boundaries
BNL-NUREG-51157 (1980)

/34/ Ginsberg, T. et al.:
Volume-Heated Boiling Pool Flow Behaviour and Application to Transition Phase Accident Conditions
BNL-NUREG-24984 (1978)

/35/ Farahat, M. et al.:
Fuel Dispersal Experiments with Simulant Fluids
Proc. Int. Meeting on Fast Reactor Safety and Related Physics
CONF-761001, pp. 1707 (1976)

/36/ Ginsberg, T.:
Role of Condensation on Dispersion of Closed Boiling UO_2 Systems
Trans. ANS 26, 363 (1977)

/37/ Rothrock, R. A. et al.:
On the Potential for Plugged Core Pressurization Following a Hypothetical Accident in an LMFBR
Nucl. Eng. and Design 53, 197 (1979)

/38/ Bell, C. R.:
A Calibration of the SIMMER-II Boilup Capability
Trans. ANS 39, 662 (1981)

/39/ Greene, G. A. et al.:
Thermo-Fluid Mechanics of Volume Heated Boiling Pools
BNL-NUREG-50759 (1977)

/40/ Gustavson, W. R. et al.:
Heat Transfer and Fluid Dynamic Characteristics of Internally Heated Pools
BNL-NUREG-21856 (1977)

/41/ Stein, R. P. et al.:
Studies of Heat Removal from Heat Generating Boiling Pools
Fast Reactor Safety Conference, Beverly Hills (1974)
CONF-740401, pp. 865

/42/ Gabor, J. D. et al.:
Heat Transfer from Heat Generating Boiling Pools
ASME-AICHE Nat. Heat Transfer Conf., St. Louis (1976), pp. 78

/43/ Fauske, H. K.:
The Role of Core-Disruptive Accidents in Design and Licensing of LMFBRs
Nuclear Safety 17, No. 5, 550 (1976)

/44/ Maschek, W. et al.:
Untersuchung von Modellfällen für Sekundärkritikalitäten im Kernbereich des SNR-300 (Mark 1A Kern)
KfK 3320 (1981)

/45/ Fauske, H. K.:
The Role of Energetic Oxide Fuel-Sodium Thermal Interactions in LMFBR Safety
Third CSNI Spec. Meeting on Sodium Fuel Interaction in Fast Reactors
Tokyo 1976

/46/ Cho, D. et al.:
Meltout of Above Steel Blockage, Laminar Film Condensation on the Underside of a Melting Surface
ANL-RDP-30, 7.3 (1974)

/47/ Chawla, T. C. et al.:
Heat Transfer from Heat-Generating Boiling Pools Pertaining to Transition Phase and PAHR
Trans. ANS 39, 666 (1981)

/48/ Greene, G. A. et al.:
Boiling Pools with Internal Heat Generation
Advanced Reactor Safety Research Division
Quarterly Progress Report
BNL-NUREG-51130, 90 (1980)

/49/ Ginsberg, T. et al.:
Hydrodynamic Characteristics of Two-Phase Dispersal Systems
Reactor Safety Research Programs
Quarterly Progress Report
BNL-NUREG 50747, 125 (1977)

VI. NOMENCLATURE

c	Heat capacity
D	Hydraulic diameter
f	Friction factor
Gr	Grashof number
h_{fg}	Heat of vaporization
j	Superficial velocity
g	Gravitational acceleration
K	Thermal conductivity
Nu	Nusselt number
Q	Volumetric heat generation rate
q	Heat flux
Pr	Prandtl number
Ra	Rayleigh number (Gr x Pr)
T	Temperature
v	Velocity
x	Penetration distance, Pool height
α	Void fraction
$\bar{\alpha}$	Average void fraction
β	Thermal diffusivity
γ	Thermal expansion
δ	Fuel crust thickness
θ	Angle to wall inclination
λ	Crust growth constant
μ	Dynamic viscosity
ν	Kinematic viscosity
ρ	Density
σ	Surface tension

Subscripts

ℓ	Liquid
v	Vapor
f	Fuel
s	Steel
mp	Melting point
C	Continuous phase
H	Heavy fluid
L	Light fluid
sat	Saturation
o	Initial